West Point Research Papers

Vertical Cavity Surface-Emitting Lasers Operating with Multiple Photonic Crystal Defect Cavities

James J. Raftery Jr.
United States Military Academy

Recommended Citation

J. J. Raftery, Jr., "Vertical Cavity Surface-Emitting Lasers Operating with Multiple Photonic Crystal Defect Cavities," University of Illinois at Urbana-Champaign, Ph.D. Dissertation, (2005).

VERTICAL CAVITY SURFACE-EMITTING LASERS OPERATING WITH
MULTIPLE PHOTONIC CRYSTAL DEFECT CAVITIES

BY

JAMES JOHN RAFTERY, JR.

B.S., Washington University in St. Louis, 1988
M.S., University of Missouri - Columbia, 1996

DISSERTATION

Submitted in partial fulfillment of the requirements
for the degree of Doctor of Philosophy in Electrical Engineering
in the Graduate College of the
University of Illinois at Urbana-Champaign, 2005

Urbana, Illinois

UMI Number: 3199119

INFORMATION TO USERS

The quality of this reproduction is dependent upon the quality of the copy submitted. Broken or indistinct print, colored or poor quality illustrations and photographs, print bleed-through, substandard margins, and improper alignment can adversely affect reproduction.

In the unlikely event that the author did not send a complete manuscript and there are missing pages, these will be noted. Also, if unauthorized copyright material had to be removed, a note will indicate the deletion.

UMI®

CERTIFICATE OF COMMITTEE APPROVAL

University of Illinois at Urbana-Champaign
Graduate College

July 27, 2005

We hereby recommend that the thesis by:

JAMES JOHN RAFTERY, JR.

Entitled:

VERTICAL CAVITY SURFACE-EMITTING LASERS OPERATING WITH MULTIPLE PHOTONIC CRYSTAL DEFECT CAVITIES
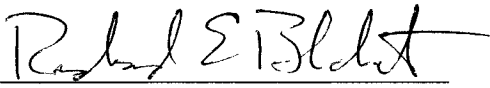
Be accepted in partial fulfillment of the requirements for the degree of:

Doctor of Philosophy

Signatures:

_____
Director of Research - Professor Kent Choquette
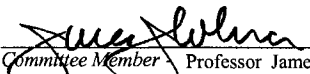
_____
Head of Department -
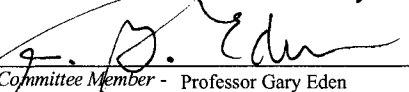
Committee on Final Examination*
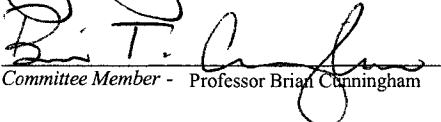
_____
Chairperson - Professor Kent Choquette

_____
Committee Member - Professor James Coleman

_____
Committee Member - Professor Gary Eden

_____
Committee Member - Professor Brian Cunningham

_____
Committee Member -

_____
Committee Member -

* Required for doctoral degree but not for master's degree

ABSTRACT

Coherently coupled arrays of vertical cavity surface emitting lasers (VCSELs) offer the potential of extended area coherent sources with high spectral purity, useful in a variety of applications in the high power (laser radar, optical communications, steerable sources) and low power (image processing, spectroscopic sensing, optical logic) regimes. A recently developed method for providing optical confinement is the introduction of a two-dimensional photonic crystal (PhC) pattern with a defect, etched into the top distributed Bragg reflector, to define a defect cavity in a VCSEL. This dissertation investigates the operation of PhC VCSELs that have multiple defect cavities to form arrays of vertically emitting lasers. A major achievement of this work is coherent coupling between the defect cavities, with both out-of-phase and in-phase coherent coupling in 2×1 and 2×2 defect cavity arrays. A qualitative and quantitative understanding of the optical characteristics of PhC VCSEL arrays was developed and demonstrated by the agreement of simulated to experiment results. Other conclusions that are supported by this study are: (1) different wafers result in coupling at different overlap integral values; (2) coupling can be effected by thermal effects (hysteresis observed), and (3) the relative phase difference between the defect civilities can be varied with injection current during both continuous-wave and pulsed operation.

ACKNOWLEDGMENTS

I am grateful to many people who have supported me in this endeavor. Special thanks go to my advisor and friend, Professor Kent Choquette. Being a member of his Photonic Device Research Group was a truly educational and rewarding experience, both professionally and personally. I must thank the many members of the research group alongside whom I have worked. I am grateful for the help of Aaron Danner, Ann Lehman, Paul Leisher, Dan Grasso, Robin Kim, Tony Giannopoulos, and Chris Long for their direct contributions to this work, as well as for the support and camaraderie of all of the group members. I would like to make special mention of two undergraduate students, Josh Sulkin and Dominic Siriani, who provided immeasurable assistance in the collection of data used herein.

I would like to acknowledge and thank the remaining members of my thesis committee, Professor Jim Coleman, Professor Gray Eden, and Professor Brian Cunningham. I would also like to thank Professor Umberto Ravaioli for serving as a member of my preliminary examination committee.

I would like to thank Dr. John Pellegrino of the Army Research Laboratory for his support of this work. I would also like to thank COL Andre Sayles and COL Barry

iv

Shoop for my selection to join the faculty of the United States Military Academy, making my opportunity to attend the University of Illinois at Urbana-Champaign possible.

Finally, and most importantly, I want to thank wife Linda who has been there for me throughout this effort. I appreciate and depend on her love and support. Thanks to our children Jeremy and Erin for being our inspiration.

v

TABLE OF CONTENTS

vi

CHAPTER 1

INTRODUCTION

1.1 Background and Motivation

In its most fundamental definition, the term photonic crystal (PhC) denotes a periodicity in optical refractive index. The concept of the PhC was first introduced in 1987 by Yablonovitch, who suggested that spontaneous emission could be completely forbidden within an electromagnetic bandgap [1]. When realized at optical wavelengths by employing a periodic dielectric media, the resulting physical structure is termed a PhC and the forbidden electromagnetic band is denoted as the photonic bandgap (PBG). The experimental verification of this concept was first carried out at microwave frequencies in 1989 [2]. This was an important achievement, as it demonstrated that the bulk properties of the light-matter interaction could be directly affected by a PhC. While Purcell had described the property of a microcavity to modify spontaneous emission more than 40 years earlier [3], it was the work by Yablonovitch that lead to the PhC becoming a topic of major research interest and opportunity.

PhCs can be realized by creating 1-, 2-, and 3-dimensional (1D, 2D, 3D) periodic variations in the index of refraction of a structure. It was discovered that 2D PhCs exhibit a PBG in the direction of their periodic index variation (perpendicular to the PhC), but not in the non-

1

periodic dimension (parallel to the PhC) [4-7]. The physical details of these structures determine their PBG. A range of light frequencies is disallowed in the PBG, analogous to the electronic bandgap that is seen in semiconductor materials. However, if one inserts an intentional irregularity (or defect) into the periodic PhC structure, photons will tend to be confined around this region. The defect has the effect of inserting a localized mode into what was the forbidden zone of the PBG, permitting photons of a particular wavelength to exist but not to propagate in the PhC. Since the use of conventional electronics fabrication technologies can be much more easily applied to the creation of 2D PhCs than to 3D PhCs, many examples of lasing 2D PhC devices have been reported [8, 9].

An example of a 1D PhC is the vertical cavity surface-emitting laser (VCSEL). The VCSEL was invented by Soda et al. in 1979 [10], though it was not considered a 1D PhC until after Yablonovitch's discovery ten years later. The VCSEL typically consists of a multiple quantum well active region as the gain medium, bounded by top and bottom distributed Bragg reflectors (DBRs) to create a resonant cavity. Population inversion is commonly provided by direct electrical injection through the doped DBR layers. Ohmic contacts can be made using Ti-Au for the p-type contact and AuGe/Ni/Au for the n-type contact. The most commonly commercially produced VCSELs emit at a wavelength of 850 nm by utilization of GaAs in the quantum wells. The DBR layers are comprised of alternating layers with high and low aluminum mole fraction of AlGaAs, with typical resultant refractive index values of 3.0 and 3.55 for the high and low Al content layers, respectively, at 850 nm. In order to achieve very high mirror reflectivities, 25 to 35 mirror periods are commonly created by epitaxial growth, with fewer mirror periods on the side of the device where light is to be coupled externally. Lateral current confinement is most often achieved by means of selective oxidation [11] of an epitaxial

2

layer or layers, or by ion implantation. The introduction of an oxide layer also introduces an index step that provides inherent optical confinement, while the use of ion implantation for current confinement provides no such index step.

VCSELs have major commercial markets, primarily as the light sources in local area networks for short-haul fiber optical data communications links. Other applications for VCSELs are optical sensing and spectroscopy, reduced-scale atomic clocks, and free-space optical interconnects. Very often it is desirable to have the highest possible light output power while maintaining single fundamental mode operation. Because of the narrow thickness of the epitaxially grown active region and cavity, VCSELs operate in a single longitudinal mode. However, unless strict attention is given to design and fabrication, multiple lateral mode operation can be the result of the relatively large optical cavity diameters. Several viable methods for achieving single fundamental mode operation in VCSELs have been demonstrated, including etched air posts [12], selective oxidation [13], ion implantation [14], surface relief etching [15], and combinations of the aforementioned [16,17]. These approaches typically involve small cavity diameters, complex fabrication procedures, and/or excessive optical loss. The desire to create a readily manufactureable and robust process to achieve high power single fundamental mode operation motivated the development of the PhC VCSEL. It has been discovered that PhC VCSELs can achieve high power single mode operation with a reproducible, simple fabrication process that is extendable to any VCSEL material system [18].

A PhC VCSEL is created when a 2D PhC pattern containing at least one defect is etched into the top DBR of an ion-implanted or selectively oxidized VCSEL [18-20]. This is schematically shown in Figure 1.1(a) and (b). Figure 1.1(c) shows that three lateral regions of effective index result: (i) the region within the defect that contains neither the PhC or oxide

3

layer, (ii) the region that contains the effect of the PhC, and (iii) the region that contains the effect of the PhC and oxide layer (dominated by the oxide layer). This index profile can produce a resonant cavity confined in the lateral dimension by the PhC, and is referred to as a PhC defect cavity. While such a 2D configuration is indeed a PhC, the laser's operation does not rely on a PBG, as the propagation and emission of light are parallel to the air holes comprising the PhC, and not in the plane of the periodic index variation introduced by the holes. This is a situation directly analogous to the PhC fiber, where a central propagation region is surrounded by a pattern of air holes extending axially along the fiber. Such an arrangement has resulted in fibers with unique single mode operation independent of operating frequency, described as an "endlessly single mode" property [21].
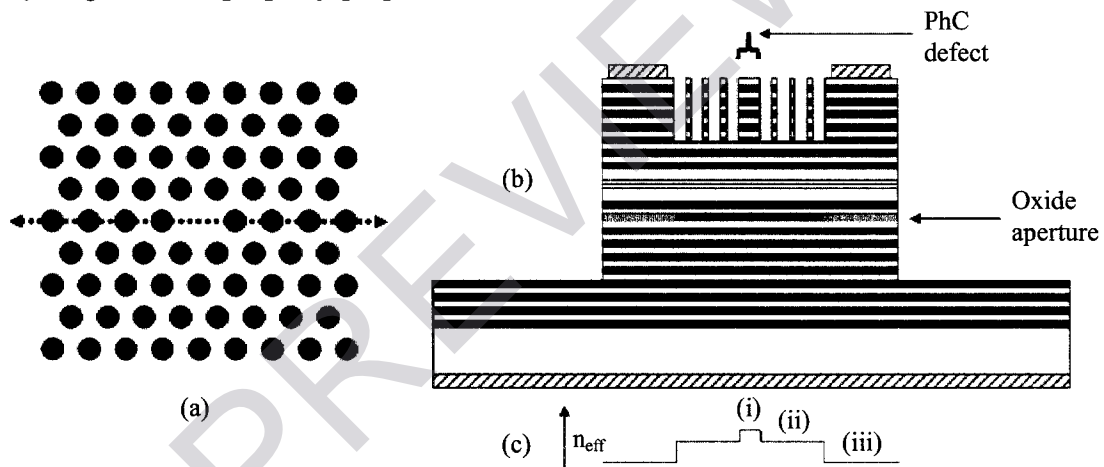
Figure 1.1: (a) Top view of a PhC pattern with a single defect. The red arrow indicates the slice shown in (b) the side view cross section of a PhC VCSEL. (c) Indicates the corresponding change in effective index seen in the structure (not drawn to scale).

To illustrate this point graphically, a photonic band diagram is shown in Figure 1.2 [22]. For this case, a perfect 2D PhC (infinite air holes with no defects) in a bulk semiconductor material is assumed. A triangular lattice with a hole diameter *(b)* to lattice constant *(a)* ratio, or *b/a*, of 0.85 was used. The shaded region marks the in-plane PBG. However, in the out-of-plane propagation case shown on the right of the plot in Figure 1.2 the bandgap vanishes, as would be

4

expected since there is no varying index in this direction. The out-of-plane photonic band diagram is useful in that it allows for the calculation of the effective index for the structure. This is done by taking the inverse slope of a straight line from the origin to its intersection with the lowest order propagating mode (denoted by the red curve) at a point fixed by the lattice constant for the particular 2D PhC pattern divided by the operating wavelength [22], analogous to the PhC fiber case [21].
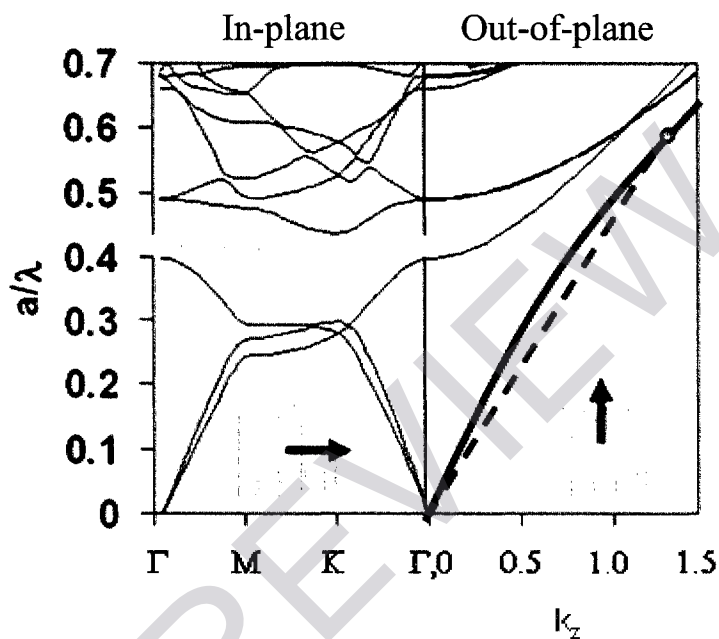

Figure 1.2: Photonic band diagram for a perfect 2D PhC modeled as infinite air holes in a surrounding bulk semiconductor material. Both the in-plane and out-of-plane (for increasing k_z) cases are shown. The in-plane PBG is indicated by the shaded region. The red curve indicates the lowest order out-of-plane propagation mode. The dashed line is used in approximating the effective index for the out-of-plane case [22].

Using this approximation to determine the refractive index of a PhC along with a transmission matrix approach, we can determine an effective index for the three regions (i), (ii), and (iii) of Figure 1.1(c), and denote them n_m, n_{eq}, and n_{ox}, respectively. The transmission matrix approach is applicable because cavity resonance wavelength shifts correspond to changes in effective index [23]. The finite depth of the PhC holes can be accommodated in n_{eq} by calculating an effective index for each DBR layer penetrated by the PhC holes before applying

5

the transmission matrix approach [18]. Experiments confirmed the validity of using such a PhC model, and showed that an average index method approach was not appropriate [24].
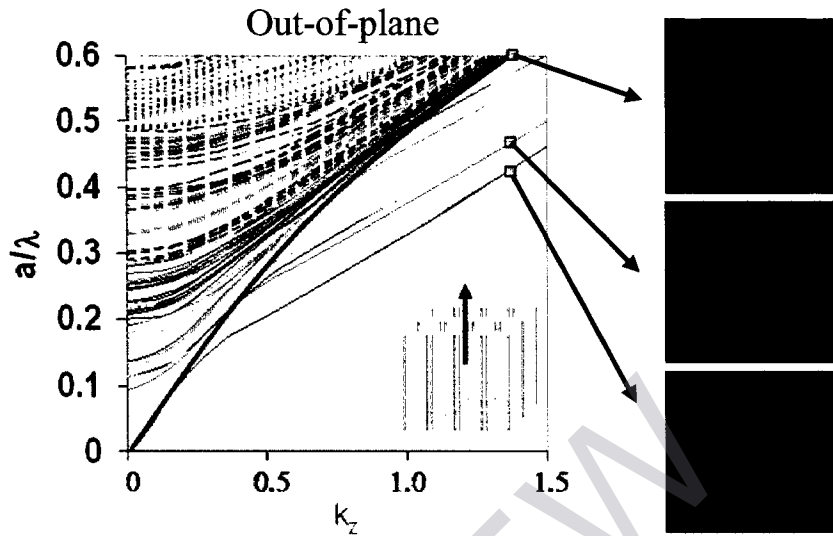

Figure 1.3: Out-of-plane photonic band diagram for a single hole defect in the previous 2D PhC. There now appear guided PhC modes lying below the red curve, which represents the lowest order radiation mode. Three calculated modal intensity plots are shown [25].

Figure 1.3 shows the resulting change in the out-of-plane photonic band diagram when a defect is added to the PhC pattern (still assumes infinite hole depth) [25]. Notice that there are now a number of modes which lie below the red curve. These are the modes that are confined and guided by the PhC defect. The two lowest order PhC VCSEL modes are shown (for $k_z =$ 1.4). The first unconfined PhC mode (also called a radiation mode) is also shown (for $k_z = 1.4$). This is a mode which is not guided by the PhC defect. The modal intensity distributions are influenced by the PhC holes, as is apparent in Figure 1.3. It is also apparent from the photonic band diagram that for $k_z > 0.4$ this is a multimode design, since more than just the fundamental PhC defect mode are confined and allowed below the unconfined mode.

A motivation for creating PhC VCSELs was the potential for engineering VCSEL modal properties. The precise control that the PhC affords in engineering the lateral index confinement,

6

not easily available with other methods used in VCSEL manufacturing, allows for the design of single mode operation which can be accomplished by use of the V_{eff} parameter [24]. The fabrication parameters that may be engineered are: (1) the PhC lattice constant a (this is the spacing between centers of nearest neighbor holes); (2) the hole diameter b; (3) the hole depth; and (4) the number of missing air holes making up the defect. Resulting spectral plots for a single mode and a multimode PhC VCSEL are shown as Figure 1.4(a) and (b), respectively [26]. The light versus current characteristic for a single fundamental mode PhC VCSEL is shown in Figure 1.5 [27]. The device achieved greater than 3 mW of continuous wave (CW) room temperature output power, with greater than 30 dB side mode suppression from threshold to maximum power. Additionally, PhC VCSELs have also shown promising results with regard to high speed small signal modulation [28].
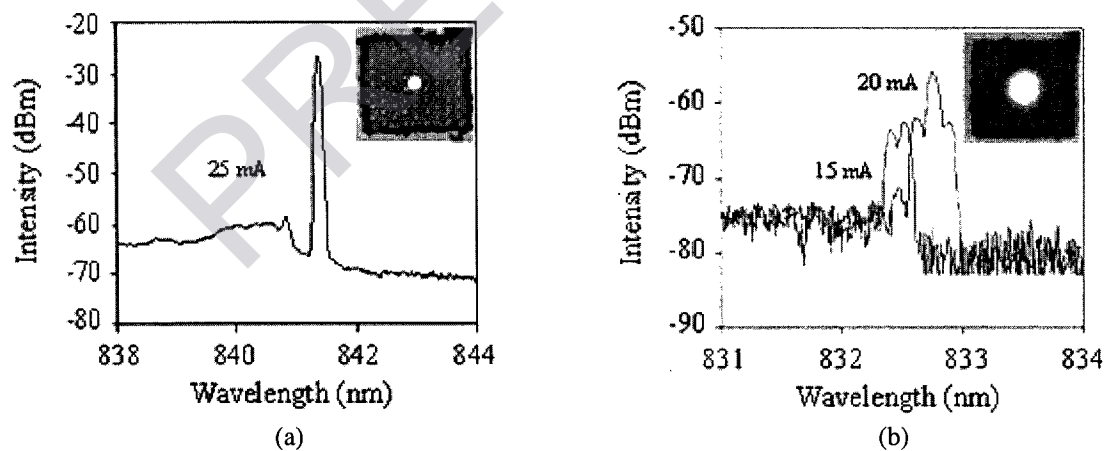

(a)

(b)

Figure 1.4: Lasing spectra for (a) a single mode PhC VCSEL and a (b) multimode PhC VSCEL. Inset are the near field images of the lasing devices [26].
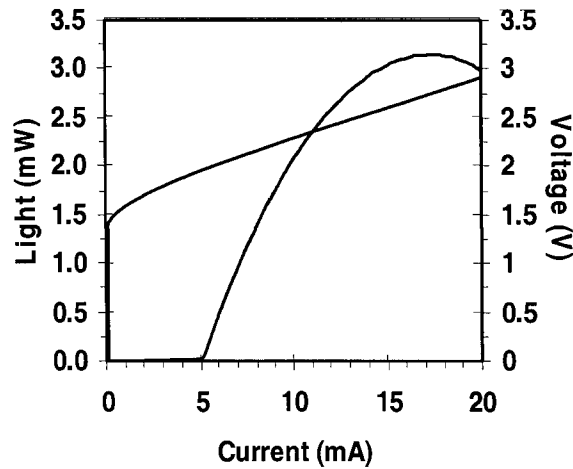
7

Figure 1.5: LIV plot for a PhC VCSEL lasing in the single fundamental mode from the threshold current value to the maximum light output current value [27].

A rigorous and thorough investigation into the modal properties of PhC VCSELs fabricated into selectively oxidized VCSELs has been conducted [18]. However, until now the far field radiation properties of the PhC VCSELs have not been examined. To that end, devices that were previously examined in [18], and determined to operate as single mode PhC defect cavity confined devices, were investigated to determine their far field emission properties. The first determination made was the appropriate current to use when observing the far field measurement. Several devices were tested by providing current injection at various levels from below threshold to above threshold and measuring the angular width of the resulting far field radiation profile.

The results for a PhC VCSEL with a single defect are shown in Figure 1.6. This plot shows the angular widths of the far field intensity pattern measured at the $1/e^2$, $1/e$, and $1/2$ times the maximum intensity points (see Figure A.1 in Appendix A for a graphical depiction explaining how this measurement convention is defined and applied throughout this dissertation). Measurements were made over a broad range of injection currents, both below and above the measured threshold current of 3.9 mA. It is seen that the angular width narrows dramatically

8

once threshold is achieved and reaches a constant value for all three measurements soon after [29]. In order to insure that future far field measurements would be taken within the range of constant angular width, 1.5 times threshold current is used as the measurement standard.
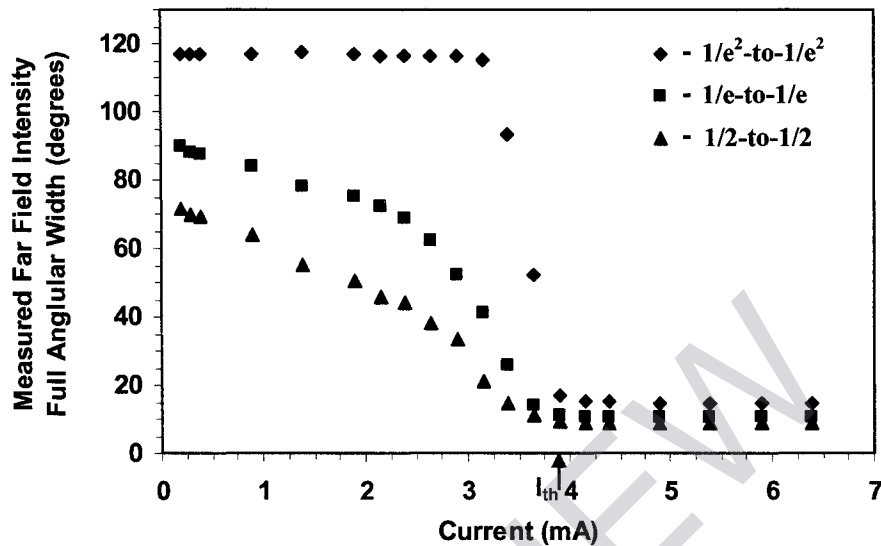

Figure 1.6: Measured full angular width of the far field intensity pattern for a single defect cavity PhC VCSEL. Measured threshold current is 3.9 mA. 0° scan was used for each data point.

Following these results, far field measurements where then made at 1.5 times threshold for many single mode PhC VCSELs of various design parameters and oxide aperture sizes. Results for three devices having PhC lattice parameter of $a = 4$ μm (this is the lattice parameter value used in the studies presented in later chapters), along with the result for a single mode selectively oxidized VCSEL fabricated on the same sample but without the addition of the PhC pattern, are shown in Figure 1.7. Scans were taken for each device along the 0° direction (an explanation of the conventions used in measuring and displaying far field data used throughout this dissertation is found in Figure A.2 in Appendix A). Gaussian fits were calculated for each device, with R-squared values ranging from 0.992 to 0.999 (an R-squared value of 1.0 equals a perfect fit). In addition to the well behaved adherence to a Gaussian fundamental mode, the most
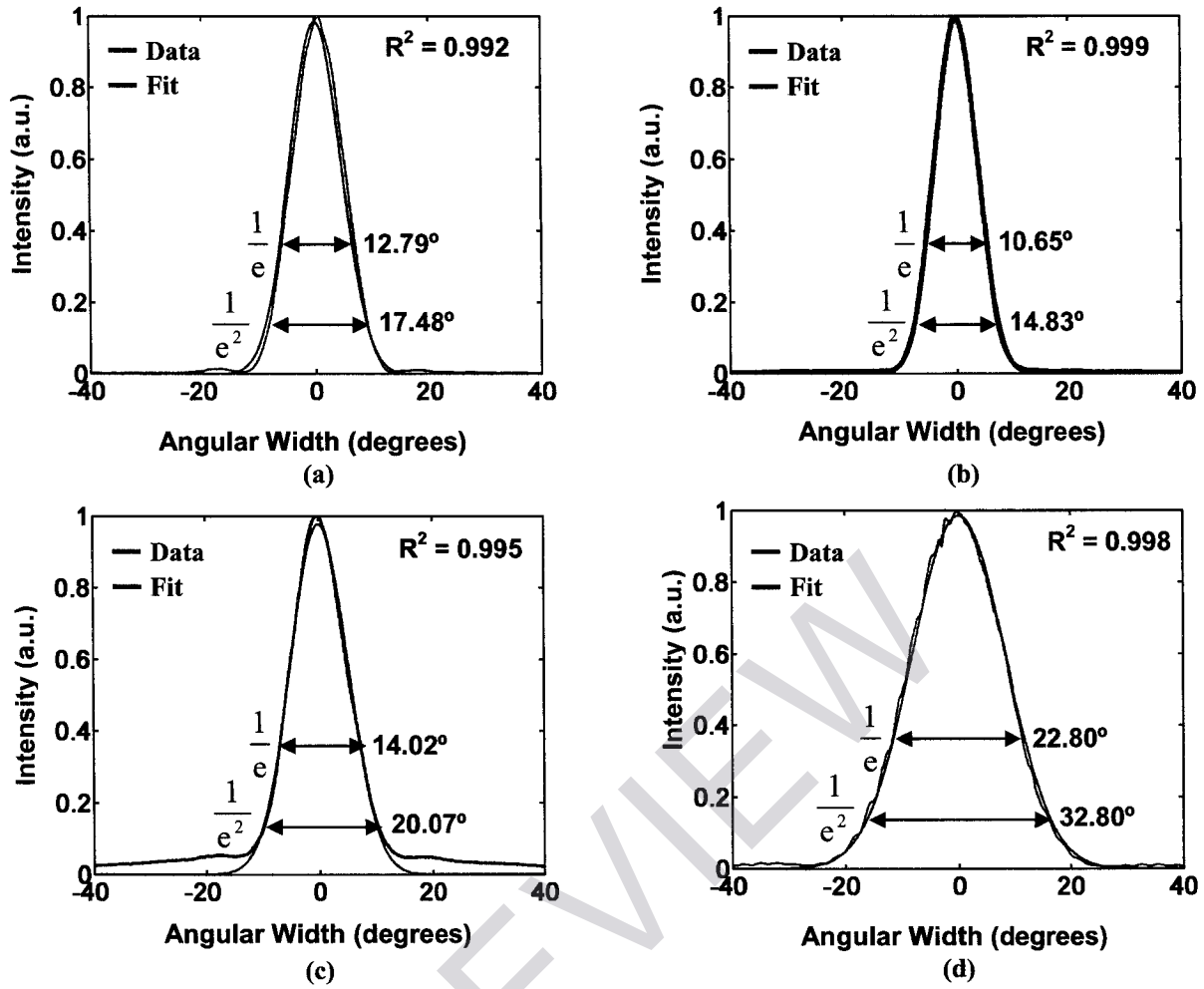
9

Figure 1.7: Gaussian curve fits to the measured fundamental mode far field intensity profiles from a PhC VCSEL with (a) $a = 4$ µm, $b/a = 0.5$, oxide aperture = 5 µm, defect diameter = 6 µm, (b) $a = 4$ µm, $b/a = 0.6$, oxide aperture = 10 µm, defect diameter = 5.6 µm, (c) $a = 4$ µm, $b/a = 0.7$, oxide aperture = 15 µm, defect diameter = 5.2 µm, and (d) a selectively oxidized VCSEL with oxide aperture = 3 µm. The R^2 value for each curve fit and the $1/e$ and $1/e^2$ full angular widths are shown. Data was collected at 1.5 times the threshold current for each respective device. 0° scan was used in each case.

noticeable result from these measurements is that the PhC VCSELs have dramatically narrower angular beam divergence than the oxide VCSELs. The oxide VCSELs tested have $1/e^2$ angular beam widths from more than 30° to more than 50°, while the PhC VCSELs are typically in the 10° to 20° range for the same measurement. This results from the same fundamental property of the PhC VCSEL that is exploited to achieve high power operation, namely the ability to increase the diameter of the lasing defect cavity while still maintaining single mode operation, which is

10

not a property of the oxide VCSEL. Since the mode size of the PhC VCSEL increases with the size of the defect cavity, the angular width of the far field, which is the Fourier transform of the near field mode, is subsequently reduced. Therefore the benefit of increasing power by increasing the defect cavity diameter also leads to the benefit of increasing the effective power available for coupling into a fiber by reducing the angular divergence of the beam.

For the three PhC VCSEL results presented, it is observed that the mode size does not scale absolutely with the PhC defect diameter. For the device result shown in Figure 1.7(a) the PhC defect diameter is 6.0 µm, but this device yields a wider far field angular width that the device of Figure 1.7(b) which has a PhC defect diameter of 5.6 µm. The explanation for this result is the difference in the size of the oxide aperture in the two cases. For the former, the oxide aperture is 5 µm, while it is 10 µm for the smaller PhC defect diameter device. The result of the oxide aperture diameter being smaller than the PhC defect diameter is to cause the mode size to be smaller than would have been the case had the oxide not been a factor.

While the PhC VCSEL scans in one dimension showed good fits to a Gaussian function, it should be expected that a mode confined within the nonsymmetric defect cavity of a triangular PhC defect cavity should not be strictly Gaussian. A verification of this is found by examining the complete far field intensity pattern shown at Figure 1.8. While the dominant central lobe is Gaussian in shape, there are also six lesser lobes arranged in a hexagonal pattern that are indicative of the lasing mode not being strictly Gaussian. A measurement of the relative power division between the main Gaussian lobe and the lesser lobes shows that more than 92% of the power is contained in the main lobe, making a Gaussian approximation for the near field mode appropriate.
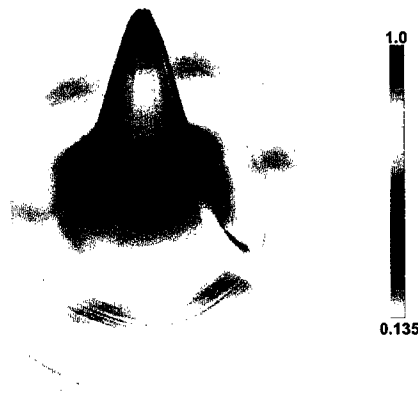
11

Figure 1.8: Measured far field intensity pattern for a single defect PhC VCSEL. The plot is rotated 20° clockwise and tilted 15° from the standard contour plot view, so that the 6 lesser lobes can be seen. 3D shadowing is provided to add contrast. (Conventions used throughout this dissertation in presenting graphical far field data are described in Appendix A.)

As an extension of the single defect cavity PhC VCSEL work, an initiative to add additional defect cavities to the PhC pattern was undertaken and is the subject of this dissertation. The goal of this effort is to achieve coherent coupling between the separate lasing defect cavities and thereby create an extended area coherent source. The benefits of achieving coherent coupling between multiple lasing elements of vertically emitting lasers has motivated this area of research for more than 15 years and offers the potential of extended area coherent sources with high spectral purity, useful in a variety of applications in the high power (laser radar, optical communications, steerable sources) and low power (image processing, spectroscopic sensing, optical logic) regimes.

1.2 Previous Work

VCSELs have several features such as low threshold, high beam quality, and low cost, which make them attractive for many applications. Because of their vertical out-of-the-epitaxial-plane light emission, VCSELs are uniquely suited for arrangement into 2D arrays. Individually

12

addressable 2D arrays of uncoupled VCSELs are potential emitters for high speed optical interconnects, such as chip-to-chip and board-to-board communications. An individually addressable 8x8 array of VCSELs was first reported in 1991 [30]. However, it is their potential utilization in coherently coupled arrays that is directly analogous to the work undertaken herein.

The first demonstration of such a phase-locked 2D array was reported in January 1990 by Yoo et al. [31]. This array was comprised of more than 160 VCSELs etched 1.3 μm in diameter, with a spacing of less than 0.1 μm between each lasing element. The overall array was 25 μm in diameter and each of the lasers was located on a 2D rectangular lattice, which allowed evanescent optical coupling between the device elements. The array produced a double-lobed beam pattern in the far field. That same year a reflectivity modulation technique was employed to produce an optically coupled 3x3 2D array of VCSELs, which also produced a double-lobed far field pattern [32].

Shortly thereafter, Hadley introduced a formalism for the investigation of optical modes of 2D phase-locked VCSEL arrays [33]. He described a fundamental and higher order evanescent mode for the case where VCSEL array elements are separated by material of lower refractive index. He also described a fundamental and higher order "leaky mode" for the case where VCSEL array elements are separated by material of higher refractive index. Because this case is not applicable to the work conducted herein, discussion will be limited to the evanescently coupled case. The fundamental mode arrangement has adjacent emitter elements of the array that are in-phase with each other; that is, the elements have zero relative phase difference. For the higher order modes, the adjacent elements are out-of-phase with each other; that is, they have a relative phase difference of 180°. Figure 1.9 shows a qualitative depiction of
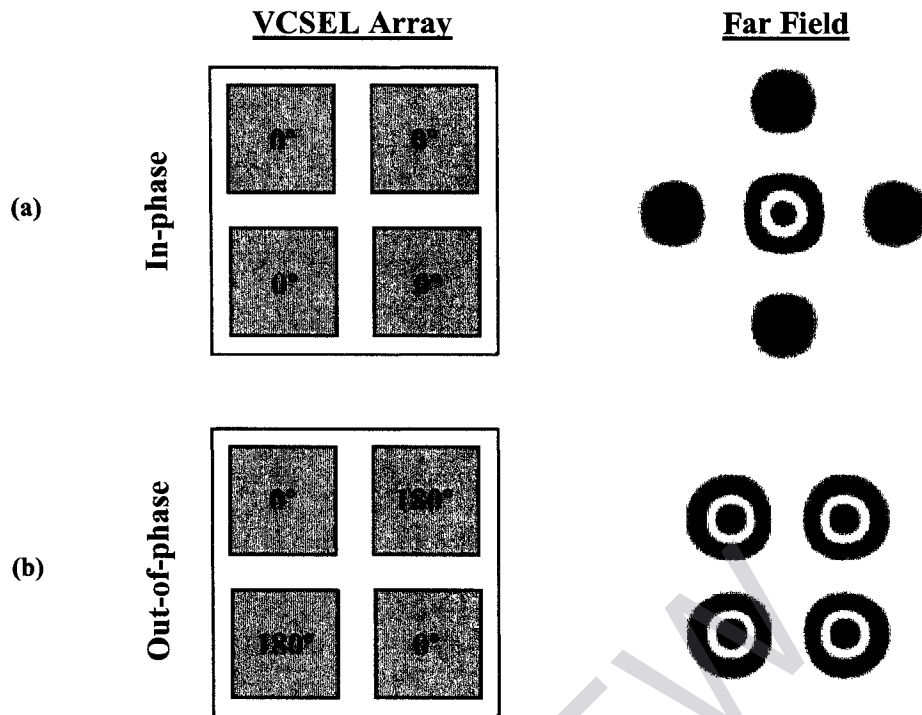
13

VCSEL Array　　　　　**Far Field**

(a) In-phase

(b) Out-of-phase

Figure 1.9: Graphical depiction of the results described by Hadley [33], for VCSEL arrays in the coherently coupled (a) in-phase and (b) out-of-phase cases. Shown at the left are gray boxes representing the top-down view of a 2×2 arrangement of VCSELs with relative phase angles labeled for the in-phase and out-of-phase cases, respectively. Also shown is a qualitative depiction of the resulting far field radiation pattern indicative of in-phase and out-of-phase coherent coupling, respectively.

the phase relationship between adjacent elements in an extended array of individual VCSEL elements as used in the calculations by Hadley, illustrating this point. For the parameters of his calculations, Hadley concluded that in the evanescent coupling case, the higher order mode would have lower loss than the fundamental mode, where the lowest loss mode is likely the mode that would occur at threshold. He also made predictions for the 2D far field profiles. The fundamental mode in the 1D array case (line array of devices) is characterized by a single on-axis lobe accompanied by two smaller side lobes. Hadley predicted that for the 2D array case, the fundamental mode should result in a central peak surrounded by four lesser side lobes, as is illustrated graphically in Figure 1.9(a). For the higher order case, the far field intensity pattern of the 1D array having two identical off-axis peaks is replaced in the 2D array case by a pattern

14

with four nearly equal off-axis peaks, as seen in Figure 1.9(b). Hadley concludes that gain-guided and most index-guided 2D arrays are likely to lase in the higher order (out-of-phase) mode with their radiation emitted into four equal intensity far field peaks. Since in-phase coupling is the result most appropriate for the applications of extended area coherent sources listed earlier, Hadley's results indicate that realizing in-phase coupling in evanescently coupled devices may not be easily achieved.

To investigate these results, Warren et al. [34] fabricated 2D coherent VCSEL arrays which employed a reflectivity modulation scheme and added an integrated phase corrector in every other element in the VCSEL array. The far field pattern for the uncorrected 2D array indeed showed the four off-axis lobes predicted by Hadley, indicative of out-of-phase coherent coupling. The phase corrected array produced a far field pattern with a central on-axis lobe and four side lobes, analogous to in-phase coherent coupling. In this case, the out-of-phase coupling was converted into in-phase coupling by the intermeshed 180°-phase shifter elements. However, this result was achieved at the expense of a very difficult fabrication process.

In 1999 a two-element phased array of antiguided VCSELs was first reported [35]. The lateral index modification required for antiguiding was achieved by modification of the cavity length in the microcavity. This required a patterned 3-nm etch performed between two epitaxial growths. Both in-phase and out-of-phase operation were achieved by varying the separation between lasing elements. In 2000, this work was extended to 4x4 arrays of in-phase and out-of-phase coherently coupled antiguided VCSELs [36]. Actively controlled methods for injection locking arrays of VCSELs through the use of a "leader" laser to seed the mode of "follower" array elements in order to achieve coherent coupling has also been demonstrated to achieve both in-phase and out-of-phase coherent coupling as observed in the far field [37].

15

Our initial investigations into PhC VCSELs with multiple PhC defect cavities showed some promising results for achieving coherent coupling between multiple lasing elements, and motivated the continued work that will be described herein. Shown in Figure 1.10 is the near field image of a PhC VCSEL with a two lasing defect cavities. Shown in Figure 1.11 is the first reported example of coherent coupling between multiple defect cavities in a PhC VCSEL [38]. Figure 1.11(a) shows an uncoupled result, so categorized by the far field intensity profile that results from the superposition of the Gaussian-like beams from each of the two PhC defect cavities. The far field intensity profile shown in Figure 1.11(b) is categorized as coherently coupled because of the interference effects that are exhibited in the far field. The result is consistent with that described by Hadley as out-of-phase coherently coupled as two main lobes with an on-axis null are observed.
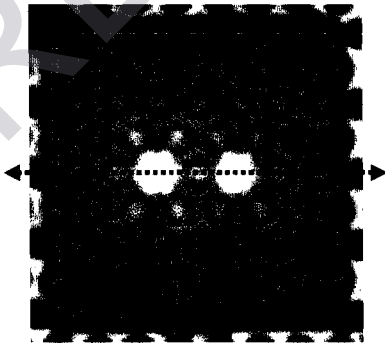

Figure 1.10: Near field image of a PhC VCSEL with multiple defect cavities each lasing in its fundamental mode. The dashed square denotes the location of the 25-µm wide oxide aperture. The red line indicates the line scanned during far field measurements [38].